



HAL
open science

Thermal assisted heterogeneous activation of peroxymonosulfate by activated carbon to degrade perfluorooctanoic acid in soil

Guanhong Liu, Jiahao Qian, Yu Zhang, Kuangfei Lin, Fuwen Liu

► **To cite this version:**

Guanhong Liu, Jiahao Qian, Yu Zhang, Kuangfei Lin, Fuwen Liu. Thermal assisted heterogeneous activation of peroxymonosulfate by activated carbon to degrade perfluorooctanoic acid in soil. *Journal of Environmental Chemical Engineering*, 2022, 10 (3), pp.107475. 10.1016/j.jece.2022.107475 . hal-03688071

HAL Id: hal-03688071

<https://hal.science/hal-03688071v1>

Submitted on 16 Jun 2022

HAL is a multi-disciplinary open access archive for the deposit and dissemination of scientific research documents, whether they are published or not. The documents may come from teaching and research institutions in France or abroad, or from public or private research centers.

L'archive ouverte pluridisciplinaire **HAL**, est destinée au dépôt et à la diffusion de documents scientifiques de niveau recherche, publiés ou non, émanant des établissements d'enseignement et de recherche français ou étrangers, des laboratoires publics ou privés.

Thermal assisted heterogeneous activation of peroxymonosulfate by activated carbon to degrade perfluorooctanoic acid in soil

Guanhong Liu ^{a,b}, Jiahao Qian ^a, Yu Zhang ^a, Kuangfei Lin ^{a,*}, Fuwen Liu ^{c,*}

^a State Environmental Protection Key Laboratory of Environmental Risk Assessment and Control on Chemical Process, School of Resource and Environmental Engineering, East China University of Science and Technology, Shanghai 200237, China

^b Univ. Rennes, École Nationale Supérieure de Chimie de Rennes, CNRS, ISCR – UMR6226, F-35000 Rennes, France.

^c School of Chemical and Environmental Engineering, Shanghai Institute of Technology, Shanghai 201418, China

*Corresponding author: Tel: +86 21 64253188

E-mail: kflin@ecust.edu.cn (KF. Lin)

* Corresponding author.

E-mail address: kflin@ecust.edu.cn (K. Lin)

<https://doi.org/00.0000/j.jece.2022.000000>

Received 00 November 2021; Received in revised form 00 February 2022; Accepted 00 February 2022

Available online 00 February 2022

0000-0000/© 2022 Elsevier B.V. All rights reserved.

Abstract: The chemical degradation of perfluorooctanoic acid (PFOA), an environmentally persistent contaminant, has recently attracted much attention. Still, very few reports have focused on the degradation of PFOA in soil due to the process's non-liquid, complex system and uneasy operation. In this study, thermal treatment was applied in the remediation of PFOA contaminated soil. Complementary to thermal activation of peroxymonosulfate (PMS), fresh activated carbon (FAC) and modified activated carbon (NAC), which were used as heterogeneous catalysts, were incorporated into the system to promote the production of sulfate radicals ($\text{SO}_4^{\cdot-}$) and the diminution of PFOA in soil. Two portions of soils, both homogenous but one with and the other without natural organic carbon (OC), were provided to study the impact of OC on the elimination of PFOA in soil. The

degradation of PFOA was initiated using the combined methods in cohesion with heat activation. During the process, the effect of temperature, the dosing amount of catalyst and oxidant, the reaction time and the volume ratio between soil and solution on the degradation of PFOA in soil were fully studied and optimized. The results showed that over a 12 h period, a PFOA (1.0 mg/kg) removal of 76% and 70% by using FAC/PMS and NAC/PMS respectively could be achieved at 60 °C. Furthermore, density functional theory (DFT) calculations were combined with experimental data and verify that the adsorption ability of both FAC and NAC for PFOA are 3 times stronger than that of soil grain. This greater adsorption can attract PFOA molecules from within soil and provide opportunities for interactions with oxidative radicals. This work sheds light on a much over-looked aspect of advanced oxidation of PFOA in soil systems, which might provide a potential option for the in-situ remediation of PFOA contaminated soil in the future.

Key words: Thermal activation, Activated carbon, PFOA, Soil organic carbon, DFT calculation

1. Introduction

Perfluorooctanoic acid, which is used extensively in both industrial production and consumer consumption [Giesy et al., 2001, Kannan et al., 2004, Jensen et al., 2008], has the ability to remain stable, for great periods of time, in the natural environment and proves difficult to be degraded even under highly extreme conditions due to the high-energy C-F bonds [Qu et al., 2010, Kennedy et al., 2004]. The vast dispersal of PFOA which is regarded as a likely carcinogen, along with its high solubility and migration advantages, makes it a substantial risk to ecological security [Lyu et al., 2018, Murakami et al., 2009]. Although it has been banned in production and utilization in accordance with the Stockholm convention of 2015 [Sorengård et al., 2019], there still remains a large remnant in underground water and soil systems. Due to its extensive use, PFOA can be found in both soil and water

environments with high concentrations having been detected especially in particular fields. For example, Sinclair et al [Sinclair and Kannan, 2006] reported that PFOA ranged from 18 to 241 ng/g dry weight in sludge from wastewater treatment plants in New York, USA. In Japan, Ahrens et al [Ahrens et al. 2010] detected that Σ PFCAs (Perfluorocarboxylic Acids) ranged from 0.29 to 0.36 ng/g dry weight in surface sediment and groundwater within landfill leachate from Tokyo, among which plume-L-PFOA recorded 1.8 $\mu\text{g/L}$. In China, Yan et al [Yan et al. 2012] found that PFOA ranged from 23.2 to 298 ng/g dry weight in sewage sludge in Shanghai, and Gan et al [Gan et al. 2010] reported that concentrations of Σ PFCAs in soils, that were greatly dominated by PFOA, ranged from 0.508 to 6.83 ng/g, with an average of 2.81 ng/g in agriculture areas in Sichuan.

Soil is what links the atmosphere and the hydrosphere, and holds a major role in the conversion and build-up of contaminants in both land-based and aquatic environments. The effective and timely removal of soil pollutants can prevent their penetration into groundwater, stop their release into the atmosphere, and/or minimize the dangerous threat they pose to the safety of living organisms [He et al., 2015, Liu et al., 2021]. Although a good deal of studies to date have been conducted to explore and strengthen the removal of PFOA in aqueous media [Yang et al., 2021, Turner et al., 2019], however only a few approaches have been developed for the degradation of PFOA in soil [Liu et al., 2021, Sammut et al., 2019, Turner et al., 2021]. Based on previous reports, the amendment of PFOA contaminated sites with carbonaceous materials (CMs) was considered advantageous as it combined carbon sequestration with pollutant immobilization. Although it is true that CMs can reduce the leachability of PFOA

and stabilize the solid material [Sørmo et al., 2020], however, the contamination in these studies were not degraded and remained present in soil; the desorption of pollutants can further cause secondary pollution [Du et al., 2014].

The synergistic behavior between granular-sized activated carbon (AC) and appropriate oxidant has been proven to be an effective method to degrade PFOA [Peng et al., 2017, Liu et al., 2015]. In situ chemical oxidation (ISCO), which has been gaining greater attention due to its effective and relatively convenient trait for the treatment of organic contaminated soil [Devi et al., 2016, Khalil et al., 2001], also demonstrates great potential to remediate the PFOA-contaminated soil. Moreover, peroxymonosulfate (PMS, HSO_5^-) which is characterized by a high redox potential, as well as good stability under normal conditions, has been gradually adopted for use in ISCO [Yun et al., 2018, Wang et al., 2018]. Therefore, further exploration on whether the combination of AC and PMS methods can be applied in the degradation of PFOA in soil, and how to improve the degradation performance of the combined methods was continued.

In addition, Sulfate radicals ($\text{SO}_4^{\cdot-}$) can be generated during the effective activation of PMS through different methods, including transition metal ions, UV irradiation, heat, ultrasonic or nanocarbons [Liu et al., 2017, Chen et al., 2015, Da Silva-Rackov et al., 2016, Qian et al., 2016]. Among these activation means, especially for soil remediation, the application of heat has been reported to activate the generation of $\text{SO}_4^{\cdot-}$ in soil to promote the removal of organic pollutants in soil [Tsitonaki et al., 2010]. In addition, an increase in temperature could separate contaminants from soil particles which can enhance the mobility

of contaminants or even turn contaminants into less toxic byproducts [Peter et al., 2018, Antoniou et al., 2010, Wang et al., 2017]. Therefore, thermal activation was adopted in this study and anticipated to enhance the oxidation efficiency on our refractory target pollutant.

The fresh activated carbon (FAC) and nitric acid modified activated carbon (NAC) which characterized by better adsorption ability and facilitate electron transfer [Liu et al., 2020], are respectively used as catalysts in this study. The possible mechanisms for the thermal-assisted AC/PMS methodology are as follows: utilizing thermodynamics for transporting pollution from soil to adsorbent and activating PMS to produce radicals which in turn attack the contaminant. The optimum usage of the catalysts and the oxidant, along with the influence factors of the reaction, were then considered. As the main component of soil, the effects of organic carbon (OC) on PFOA degradation, a rarely discussed topic in soil remediation, were also investigated in this study. Finally, the density functional theory (DFT) calculations were conducted based on the experimental data to verify the elimination mechanisms of PFOA in soil by using FAC/PMS and NAC/PMS. The obtained research conclusions can provide useful information for the chemical oxidation remediation of PFOA contaminated soil and provide a feasible method in practical application.

2. Materials and methods

2.1 Chemicals and reagents

PFOA was acquired from Aladdin reagent Co. Ltd. Isotope-labeled internal standards including PFOA, $C_6F_{13}COOH$ (PFHpA), $C_5F_{11}COOH$ (PFHxA), C_4F_9COOH (PFPeA) and C_3F_7COOH (PFBA) were purchased from Wellington Laboratories (Guelph, ON, Canada).

Potassium peroxymonosulfate (PMS) was from Meryer Chemical Technology Co., Ltd. The activated carbon (AC) (diameter: 4 mm, height: 6 mm) was purchased from Macklin Biochemical Co., Ltd (Shanghai, China). The nitric acid modified carbon (NAC) was obtained by immersing FAC in concentrated HNO₃ using a microwave hydrothermal method. Methanol (CH₃OH, 99.9%) and ethanol (C₂H₅OH) were Optima grade solvents for Liquid Chromatography-Mass Spectrometry (LC/MS) analysis were acquired from Sinopharm Chemical Reagent Co., Ltd. (Shanghai, China). Solution pH was adjusted by HCl (0.1 M) or NaOH (0.1 M). Ultrapure water from a Milli-Q water process (Classic DI, ELGA, Marlow, UK) was used in preparation of aqueous solutions. All reagents were used without any purification.

2.2 Soil sample preparation

Uncontaminated soil was collected from a depth of 0.25-0.35 m at a site in East China University of Science and Technology in Shanghai, China. The soil was air-dried at room temperature, large stones and plant residues were removed, and then passed through a 2 mm sieve. The soil was characterized as follows: 6.1% clay, 28% silt and 65.9% sand, pH 6.5, 3.42% organic matter. For the experiments, a set of spiked soil samples was prepared according to our previous method [Peng et al., 2017]. Clean soil and spiked soil (with 20 mg/L of PFOA stock solution) at a volume ratio of 1:1 were placed in a 1000 mL beaker. The combined soil was then stirred vigorously with a glass rod to promote homogeneous distribution of PFOA, after which the spiked soil was placed in a fume hood. Finally, the soil was aged for 1 month in darkness at room temperature (20 °C) before any treatment in the

laboratory. In order to study the function of organic carbon in soil during the in situ remediation, soil was heated in a muffle oven at 600 °C for 6 h to remove the OC and labeled as soil-600 as a contrast.

2.3 Soil sample extraction

To extract the PFOA from the solids, a previously reported method was used as a base and modified accordingly [Chen et al., 2016]. 1.0 g of soil sample was weighed and placed into a 50 ml polypropylene centrifuge tube. To the tube, 5 mL methanol was added, vortexed for 1 min, and allowed to stand for 10 min. After standing, the tube was ultrasonicated at 40 °C for 20 mins, then centrifuged at 3500 r/min for 10 mins, the produced supernatant was then placed in a new centrifuge tube. The above extraction process was repeated two more times, collecting a total of 15 mL of supernatant. Afterwards, the supernatant was blown under a gentle flow of high-purity nitrogen to achieve a 1-2 mL concentrated extract which was then diluted with 50 mL ultrapure water.

Before the extract was injected into the WAX column for purification and extraction, the column was activated using a mixed solution (4 mL methanol, 4 mL 0.1% ammonia in methanol and 4 mL ultrapure water), and the effluent discarded. 50 mL of the extract was then added into the activated cartridge. After the solution was allowed to flow out, the cartridge was washed with a mixture of 10 mL of ultrapure water and 4 mL of 25 mM ammonium acetate (sodium acetate). All solutions were not preserved. Finally, the cartridge was eluted with 4 mL methanol and 4 mL 0.1% ammonia methanol solution. The 8 mL of eluate was collected using a 15 mL polypropylene tube, blown to near dryness under a gentle high-purity

nitrogen stream, re-diluted to 2 mL methanol, vortexed for 30 s, and passed through a 0.22 μm membrane before being tested. The extraction efficiency of PFOA in soil was put in Table S1.

2.4 Procedures of degradation experiments

PFOA degradation tests were conducted in 250 mL conical flask reactors and were settled in a digital water bath oscillator at the desired temperature. Three sets of systems in which AC, PMS, AC/PMS were separately added to the reactor with contaminated soil were conducted and compared. At the beginning of the preliminary experiment, 1 g contaminated soil was added to the reactor followed by 10 mM PMS and 4 g/L AC, the reaction was then initiated by heat. After the optimization of the dosage of catalysts and oxidant, a given amount of 1 g soil, AC (8 g/L) and PMS (15 mM) were set with the ratio of soil/solution at 1.0 g/1.0 mL. The effects of pH, impact factor and the solid/solution ratio were then investigated by varying the solution pH (3-11), ion concentrations (1 and 10 mM) and the solution volume (1, 2 and 3 mL), respectively. At each designated time interval, extractions were taken from the soil samples and filtered through 0.22 μm membranes, then transferred into auto-sampler vials for quantitative analysis. The system pH was left unadjusted in all tests except when investigating the influence of the initial soil pH. Replicate runs were carried out twice for each test, and the relative standard deviations were determined to be less than 8.0%. The removal efficiency of PFOA (R_{PFOA}) was calculated from Eq 1, where C_0 and C_t are concentrations of PFOA at initial and fixed reaction times, respectively.

$$R_{\text{PFOA}} = \left(1 - \frac{C_t}{C_0}\right) * 100\% \quad (1)$$

2.5 Analytical methods

During the catalytic oxidation process, the concentrations of PFOA and its degradation products were determined by high-performance liquid chromatography combined with tandem mass spectrometry (HPLC-MS/MS) as demonstrated by Liu et al [Liu et al., 2021]. The limit of detection (LOD) of PFOA is 9 $\mu\text{g/L}$. The LOD of short-chained PFCAs and more detailed information are summarized in Table S2.

The quantitative analyses of fluorine anion (F^-) was performed by ion chromatography (ELCD ICS-1000, USA). The injection volume was 10 μL and a flow rate of 1 mL/min was used for the anion separation. The mobile phase was 9.0 $\text{mM Na}_2\text{CO}_3$ and the flow rate was 1.0 mL/min [Köster et al., 2019]. By calculation, the LOD of F^- is 1.113 ppb at a signal-to-noise (S/N) ratio of 3, the specific measurement can be found in SI.

2.6 Computational Details

DFT calculations were performed using the DMol³ program package in Materials Studio, in which a double numerical polarization (DNP) basis set was used [Delley, 2020]. The Perde-Burke-Ernzerhof (PBE) functional within the generalized gradient approximation (GGA) [Hammer et al., 1999] was applied to describe the electron exchange-correlation function. The total energy, maximum displacement, and maximum force tolerances were converged at 2×10^{-5} hartree (Ha), 5×10^{-3} Å, and 4×10^{-3} Ha/Å, respectively. The Methfessel-Paxton method [Methfessel et al., 1989] was adopted in the calculations with a Fermi smearing width of 0.001 Ha and the total energies were extrapolated to 0 K. The Brillouin zone was sampled by a $3 \times 3 \times 1$ Monkhorst-Pack k-point mesh [Chadi, 1977]. The adsorption energy E_{ads} is defined as Eq 2:

$$E_{\text{ads}} = E_{\text{adsorbate/slab}} - E_{\text{slab}} - E_{\text{adsorbate}} \quad (2)$$

where $E_{\text{adsorbate/slab}}$ represents the total energy of adsorbate and slab, $E_{\text{adsorbate}}$ refers to the energy of PFOA, E_{slab} means the energy of clean surface, respectively. The distance between surfaces and adsorbed PFOA molecule was also measured after the structural optimization.

3 Results and discussion

3.1 Degradation optimization

3.1.1 Effect of temperature

Though heat is an effective way to activate PMS [Hori et al., 2008], however, there was a notable limitation for sole PMS on the removal of PFOA at elevated temperatures (Fig. S1). Therefore, the influence of temperature as a crucial activation factor on the removal of PFOA by the combination of FAC/PMS or NAC/PMS was investigated through heterogeneous catalytic reactions in soil. Fig. 1 illustrates a 18% and 34% removal of PFOA by FAC/PMS and NAC/PMS at room temperature, respectively. By raising the temperature, the removal efficiency of PFOA was improved to 33% and 47.5% by FAC/PMS and NAC/PMS at 60 °C. The results prove that a higher reaction temperature not only has a strong influence on PMS decomposition, but can also improve the diffusion rate of the catalytic molecules across the external boundary layer and within the pores [Forouzesh et al., 2019]. However, when the reaction temperature was increased to 80 °C, no significant enhancement of PFOA removal could be seen. In view of the minimal improvement affected by temperatures beyond 60 °C, it can be surmised that elevated temperatures (> 60 °C) can only enhance the removal rate of PFOA to a small degree in soil as a result of heat loss due to heat transfer between further distances. In addition, the higher temperatures may also alter many soil properties such as

water content which can affect the capacity of certain soil functions (Table S3). Besides, for soil remediation, the increase of temperature can limit the transport of PS in soil, thereby affecting the removal of organic pollutants [Tsitonaki et al., 2010]. Hence, 60 °C was chosen as the optimum temperature to carry out all experiments in our study.

Fig. 1.

3.1.2. Effect of PMS concentration

Firstly, the degradation of PFOA in soil was conducted in the presence of PMS alone which was anticipated to produce strong oxydic radicals. As depicted in Fig 2a, the highest removal efficiency of PFOA in soil was 15% when the dosage of PMS was 10 mM. With the increasing concentration of PMS from 10 to 40 mM, however, there was no remarkable improvement or reduction seen during the degradation of PFOA in soil. The removal efficiency of PFOA reached just 7% even though the PMS concentration was raised to four times its initial volume. It was assumed that a higher PMS dosage would lead to a larger generation rate of both $\text{SO}_4^{\bullet-}$ and $\bullet\text{OH}$ in solution (Eqs. (3-5)) which would in turn improve PFOA removal (Fig.S2) [Qi et al., 2019, Wang et al., 2020], however in this experiment that proved not to be the case. Unlike in aqueous solution, the excess $\text{SO}_4^{\bullet-}$ produced by aggregation in soil could not be consumed by attacking PFOA, this lead to a mutual quench phenomenon during the degradation of PFOA and resulted in a notable decrease in PFOA removal efficiency despite the increased PMS concentration. For soil-600, the degradation rate of PFOA was increased slightly from the initial 8% to 16% with the addition of more PMS. This may be the result of absent OC from the soil providing more spaces for radicals to

occupy and a smaller consumption of PMS. Nevertheless, the obtained results imply that the dispensed PMS was unable to oxidize the pollutant due to blocking from the soil particles. This may also reduce the activation energy of the reaction due to the particles adsorbing some portion of heat, resulting in the transference of less energy.



3.1.3 Removal of PFOA by FAC and NAC

The PFOA removal capacity of both FAC and NAC were determined using heat without the addition of PMS. As shown in Figure 2b and 2c, a noteworthy advance in the removal rate of PFOA with the rising addition of FAC or NAC in soil is observed. Although the surface area of FAC is twice that of NAC (Table. S4), there was no obvious difference in their capability to adsorb PFOA. The removal rates of PFOA were increased from 30% to 45% and from 33% to 37% with the addition of FAC and NAC from 4 g/L to 12 g/L, respectively. The adsorption amounts of PFOA from soil were 4.28, 5.06 and 6.13 mg/g with the addition of 4, 8 and 12 g/L FAC, and were 4.50, 4.75, 4.73 mg/g with the same quantities of NAC. The adsorption ability of FAC was 0.0052 mg/m^2 , which was five times higher than NAC. In the meantime, for soil-600, an obvious increase in PFOA removal, from 30% to 47% and from 30% to 39%, could be seen after the addition of FAC and NAC from 4 g/L to 12 g/L, respectively.

As observed in Fig. 2d, adsorption did not immediately occur after the injection of FAC or NAC. During the first 1-3 hrs, there was little PFOA removed from the contaminated soil,

however after 5 hrs of reaction a noticeable diminishment of PFOA in soil could be detected, indicating that contact between the PFOA from soil particles and the catalysts requires some time and the contact between FAC or NAC and PFOA in soil is a rate-limited and crucial step. Meanwhile, with the extending reaction time, the PFOA removal rate was higher in soil-600 than in soil as a result of the loss of the OC in soil Organic carbon can provide more adsorption sites for PFOA in soil through hydrophobic interaction, ligand bridging and electrostatic interactions. Without OC, the binding strength between PFOA and soil-600 was not as strong as that of PFOA and soil, indicating that PFOA-contaminated soils with less OC content can be more readily repaired by adsorbents. Afterwards, the experiments were carried out at a constant dosage of PFOA (1.0 mg/kg), PMS (15.0 mM), FAC or NAC (8.0 g/L) with a reaction time of 6 h in the initial soil system.

Fig. 2.

3.2 Evaluation of catalytic oxidation performance

3.2.1. Effect of reagent volume

Contamination in low-permeability soil poses a significant technical challenge to in-situ remediation efforts, primarily due to poor accessibility to the contaminants and difficulty in uniform delivery of treatment reagents. In order to increase the contact area between pollution in soil and chemical reagent so as to achieve a better degradation effect, the soil and solution volume ratio was adjusted and compared. As the volume ratio increased from 1 mL to 3 mL with 1.0 g soil (Fig. 3a), the increased solution volume failed to improve the removal rate of PFOA. This may have been caused by more water molecules dispersing the catalyst and

oxidant in aqueous states instead of promoting them within the soil medium.

3.2.2. Effect of reaction time

As discussed in 3.1.3, a prolonged reaction time could provide more opportunity to create better contact between PFOA and catalysts, hence the reaction time was further extended to investigate the removal rate of PFOA in soil using the combined method. As shown in Fig. 3b, the degradation efficiency of PFOA continuously increased with increasing reaction time. After 12 h, the degradation rate of PFOA reached as high as 70% and 76% for soil/FAC/PMS and soil-600/FAC/PMS, and 60% and 79% for soil/NAC/PMS and soil-600/NAC/PMS, respectively. For the advanced systems of both FAC/PMS and NAC/PMS, the degradation of PFOA was better in soil-600 than in soil. This performance difference can be ascribed to the absence of OC in soil-600 which lowered PMS consumption, and allowed more $\text{SO}_4^{\cdot-}$ and $\cdot\text{OH}$ to directly attack PFOA during the remediation process. The results also indicate that a prolonged time did indeed enhance the contact between contaminant and materials in soil.

Fig. 3.

3.2.3. Effect of systematic pH

The effect of pH on PFOA removal in soil based on AC/PMS was conducted using various pH values. In Fig. 4, for FAC/PMS, PFOA is shown to be preferably removed when under acidic conditions rather than alkaline, and can be ascribed to the transformation of $\text{SO}_4^{\cdot-}$ to $\cdot\text{OH}$ (Eq. (5)) under alkaline conditions. However, there was no significant difference in PFOA removal in soil in the presence of NAC/PMS among various pH values, indicating

that the NAC/PMS system was less affected by pH. Unlike in aqueous solution systems, there was approximately a 20% difference between the degradation of PFOA by AC/PMS under acidic conditions and in alkaline solution [Liu et al., 2020], however, no obvious distinction (< 10%) of PFOA removal could be observed by the advanced oxidation methods in soil systems. For PMS-based AOPs, PMS inevitably acidifies the treated water matrix (Eq. (4)), while the structure of the aggregated soil can contain a certain amount of weak organic acids, both of which can act as a good balance to the pH. Therefore, the pH of the soil system was not immediately changed when the PMS solution was initially injected into the reactor, thereby having no significant effect on further generation of $\text{SO}_4^{\bullet-}$. And, in turn, may also counteract any rate decrease due to PFOA protonation. Hence, this remediation method can be easily implemented under a variety of soil pH conditions.

Fig. 4.

3.2.4. Effect of co-existing matter

Several matters including chloride anion (Cl^-), bicarbonate anion (HCO_3^-), nitrate anion (NO_3^-), sulfate ion (SO_4^{2-}) and phosphate anion (PO_4^{3-}), and humic acid (HA) that exist in natural ground water and soil may affect the reactivity of AC and PMS in PFOA removal. The effects of these compositions on PFOA transformation are presented in Fig. 5a and Fig. 5b. The results illustrate that the presence of SO_4^{2-} and Cl^- had a relatively slight influence on the decomposition efficiency of PFOA by AC/PMS. In contrast, with increasing ionic concentration, the presence of HA had the most prominent, negative impact on PFOA elimination for both FAC/PMS and NAC/PMS. The inhibitory effect of HA on PFOA

degradation can be attributed to the scavenging effect (Eq. (8)) and the competition of reactive radicals with PFOA [Song et al, 2019, Li et al 2021]. Furthermore, the presence of PO_4^{3-} had a positive effect on $\text{SO}_4^{\bullet-}$ induced oxidation in AC/PMS, which could be caused by the produced $\text{PO}_4^{\bullet-}$ radicals (Eq. 13), as well as the addition of phosphate playing a promoting role in the PMS activation. [Duan et al., 2021]

In addition, with an increasing CO_3^{2-} concentration, PFOA transformation was initially facilitated and then inhibited for AC/PMS. This was most probably caused by the bicarbonate reacting with peroxymonocarbonate ions (HCO_4^-) to produce $\text{CO}_3^{\bullet-}$ radicals. These $\text{CO}_3^{\bullet-}$ radicals can be further transformed into $\text{CO}_2^{\bullet-}$ (Eqs. (9-12)) [Jiang et al., 2018], which could be beneficial to PFOA degradation. Since HCO_4^- known as a weak oxidant can be produced with the increasing of HCO_3^- and with the extending time, it would further prevent PFOA from degrading. Conclusively, the degradation of PFOA by the combined method functioned in a relatively stable way and was not easily disturbed in the soil system.

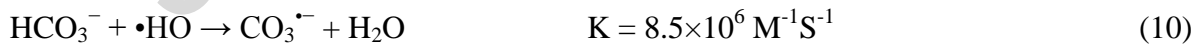


Fig. 5.

3.3. The defluorination of PFOA

Along with PFOA degradation, the defluorination of PFOA in the FAC/PMS and the NAC/PMS processes were crucial points for experimental analysis. The F^- could be detected in both the reaction solution and the soil extraction solution after the degradation of PFOA. As depicted in Fig. 6a, in each system, the F^- concentration increased continuously over time, implying that mineralization and defluorination were significant sources of decomposition for PFOA in the two systems. According to the obtained F^- concentration in soil and in liquid, the defluorination rates of PFOA accounted for 24.29% and 30% after the 12 h time period. Significantly, in terms of PFOA defluorination, FAC/PMS which had a better removal performance, was inferior to NAC/PMS. This may be a result of the surface of NAC containing more defects which allows for greater electron transfer between NAC and PMS during the decontamination process. This phenomenon is consistent with FAC and NAC degradation performance in aqueous systems.

Furthermore, based on the interpretation of HPLC-MS/MS (Fig. S3), $C_6F_{13}COOH$ (PFHpA), $C_5F_{11}COOH$ (PFHxA), C_4F_9COOH (PFPeA) and C_3F_7COOH (PFBA) were the main detectable daughter products during the degradation of PFOA. Their total concentration shown in Fig. 6b, increased at the beginning as a result of the breakdown of PFOA and then decreased as the degradation proceeded. The concentration of these products finally amounted to 0.071 mg/L and 0.108 mg/L in the FAC/PMS and NAC/PMS systems respectively, after 12 h. Then, according to the mass balance equation ($n_{F^-} + n_{undegraded\ PFOA} + n_{short-chained\ PFOA}$), the mass balances of F acquired in 12 h were 42.8 % and 58.3 % for FAC/PMS and NAC/PMS,

respectively. It was noteworthy that the obtained total mass balance of F contains the target values both in soils and in liquids, because the decomposed compounds from soils were likely to dissolve in liquids. The corresponding, remaining percentage 57.2% and 41.7% could roughly represent the PFOA absorbed on soil and AC, respectively.

As for soil-600, even though the removal rates were higher than those in soil no matter for FAC/PMS or NAC/PMS system with the prolonged time, the defluorination efficiencies in soil-600 were lower than the values achieved in soil. Due to OC being converted into CO₂ during the burning process, soil-600 may have adsorbed more PFOA during the removal process, thereby causing difficulty for radicals and electrons to attack the protected interior PFOA molecules. In comparison, the negatively-charged PFOA can adsorb onto the surface of soil due to electrostatic attraction with positively-charged OC. Because of more exterior PFOA being prone to attraction in soil, this can lead to a higher defluorination efficiency during the adsorption process.

Fig. 6.

3.4. Possible mechanism on PFOA removal

3.4.1. The FTIR and HPLC-MS/MS information of PFOA degradation in AC/PMS processes

The FTIR spectra and LC-MS/MS interpretation were joined to properly analyze the PMS/AC/PFOA interactions. Take FAC for example, the primitive FAC and soil were tested and compared with the solids (the mixed soil with FAC) after reaction. In Fig. 7, after exposure to PFOA, due to the electron withdrawing effect of the fluorinated tail on the carbon double bond, the bands of CH₃ and CH₂ of FAC which appear at 2930 and 2857 cm⁻¹ were

weakened. The association with AC was possibly caused by electrophilic character along the C-F bonds and nucleophilic behavior perpendicular to these C-H stretching vibrations bonds [Wang et al., 2019]. The characteristic absorption peaks of soil at 1080 and 800 cm^{-1} decreased after the reaction, implying that PFOA might also be partially bound to Si-O of soil. In addition, the weakened peak at 3450 cm^{-1} in NS/FAC indicates that the -OH groups on the surface of FAC and soil act as the main hydrogen bond donors to attract PFOA. Furthermore, with the emergence of C-F bonding at 1000-1400 cm^{-1} and a new peak observed at 1723 cm^{-1} , attributed to the carboxyl group of PFOA, it reveals that most PFOA molecules existed in the form of carboxylic acid and were bonded in the solid. In the meantime, the deprotonation of PFOA could cause the dissociation of hydrogen bonding between PFOA and PMS, leading to the appearance of the symmetric stretching (vs) peak of SO_4^{3-} shown at 1108 cm^{-1} . Thus, it could also be postulated that FAC can anchor the PFOA and PMS in ternary mixtures and the whole interaction mode can be carried out harmoniously.

Fig. 7.

Furthermore, the decomposition of PFOA by catalytic oxidation took place in the presence of AC and PMS upon heating. According to the data obtained from HPLC-MS/MS (Fig. S3), it was presumed that $\text{C}_7\text{F}_{15}\text{COOH}$ may be destructed to $\text{C}_7\text{F}_{15}\text{COO}^\bullet$ and then $\text{C}_7\text{F}_{15}^\bullet$, with the attack of $\text{SO}_4^{\bullet-}$ produced from PMS decomposition catalyzed by AC main pathway, $\bullet\text{OH}$ accompanied with $\text{SO}_4^{\bullet-}$ also played a vital role for the formation of $\text{C}_7\text{F}_{15}\text{OH}$. A series of intramolecular rearrangements proceed and $\text{C}_6\text{F}_{13}\text{COO}^-$ was generated through hydrolysis. The same reactions between $\text{C}_6\text{F}_{13}\text{COO}^-$ and $\text{SO}_4^{\bullet-}$ occurred as those of $\text{C}_7\text{F}_{15}\text{COO}^-$ and

converted to shorter chain PFCAs. The $C_nF_{2n+1}COO^\bullet$ was unstable and could be readily decomposed to $C_{n-1}F_{2n-1}^\bullet$ and CO_2 , and to release H^+ for a decrease in pH. This subsequently produced shorter-chain PFCAs which followed the same CF_2 unzipping cycle with sufficient oxidant until they were mineralized, allowing AC/PMS to complete the defluorination of PFOA.

3.4.2. Computation of PFOA elimination.

The degradation of PFOA by AC/PMS in soil is a complex process involving several reaction steps. The most important step during the process of PFOA remediation in soil is that AC could efficiently attract and concentrate PFOA molecules present in contaminated soil, which would be beneficial for the next catalytic oxidation. However, the adsorption ability of soil, activated carbon and modified activated carbon have not been verified because the degradation path of adsorbed substances at different interfaces is vastly complex and rarely reported on. DFT calculations were employed to examine the reliability of the proposed pathway systematically and identify the adsorption effect.

The results obtained for the optimized structures of SiO_2 , graphene and graphene with amino groups are reported in Fig. 8, which represent the soil, FAC and NAC and provided three different adsorption scenarios with PFOA [Yuan et al., 2020; Zhang et al., 2019]. For the structures of soil, silica as a main component was chosen to simulate soil and the lattice plane of 011 was selected in the calculation according to the XRD result (Fig. S4). The molecular structures of NAC owning planar conformation with amino groups were based on the FTIR information. Two conformations of PFOA were presented on each surface in order to get more

comprehensive information, and the values in parentheses were determined in soil medium.

The DFT calculations indicated that no matter the form of AC, the adsorption strength of all are much stronger than SiO_2 , and the relative adsorption strengths of PFOA were $\text{FAC} > \text{NAC} > \text{SiO}_2$. The combining energy between SiO_2 and PFOA was -8.5 kcal/mol, while the average value of FAC and NAC was -22.2 kcal/mol and -24.65 kcal/mol, respectively, which was 3 times higher than the values obtained from soil and PFOA. It implies that AC could strongly adsorb PFOA even in solid media and PFOA would not be easily released into soil again once it was bonded onto the surface of AC. The results were in line with the above experimental phenomena.

Besides, the distances between FAC and PFOA were smaller than those for NAC and SiO_2 , which provided an advantage to attract PFOA. It is well known that the molecular size of PFOA is $11.7 \times 3.95 \times 3.7$ Å, and a media with a higher micropore and a lower mesopore volume will supply the available pores for PFOA removal. Therefore, the transformation from micropores to mesopores after the HNO_3 treatment lead to a further distance between NAC and PFOA. However, the obtained amino group of NAC preferentially reacted with the carboxylic acids of PFOA where the distance between the two was around 2.34 Å, which compensated for the decline of micropore volume of NAC. Furthermore, according to the comparison of the distance, we deduced that, the most appropriate adsorption sites between PFOA and AC were the carboxyl group of PFOA with the carbon surface of FAC or NAC and with $-\text{NH}_2$ of NAC. As for SiO_2 , the C-F bond expressed tendency to bond with the Si-O-Si of soil. The deduced outcomes based on the DFT calculations corroborate with the FTIR

results. These outcomes elucidate that FAC and NAC could efficiently adsorb PFOA from soil due to the stronger adsorption energy and more stable combination. Finally, the shorter distance and less bonding energy were also beneficial for electron transport between the adsorbent and pollutant during the mineralization of PFOA by FAC/PMS and NAC/PMS.

Fig. 8.

4 Conclusions

The primary benefit of thermal treatment in soil is the speed at which remediation can be controlled, allowing for radicals to be generated from PMS in a sustainable release. PMS dissociation by heat to generate $\text{SO}_4^{\bullet-}$, in combination with these AC varieties, was anticipated to fully degrade and defluorinate PFOA. For the degradation of PFOA in soil, fewer remarkable observations of PFOA diminution using oxidant alone were noted. Although, in the sole presence of activated carbon, very limited PFOA removal could be detected due to the concentration effect though a longer contact time was required. Such results were attributed to the refractory property of PFOA and poor contact between the pollutants and reagents in soil. Compared with the removal rates of PFOA in aqueous systems, although the degradation efficiency in soil was obviously slower and lower, the addition of both catalyst and oxidant and the prolonged reaction time still enhanced the degradation performance when using FAC/PMS or NAC/PMS. The variability of organic carbon contents in soils from different regions also demonstrated a certain influence on PFOA degradation in soil. High OC is likely to immobilize the PFOA but will result in a lower PFOA elimination by the consumption of $\text{SO}_4^{\bullet-}$ during the treatment process. However, the aggregate soil structure

exhibited a distinct advantage where it presents buffering properties against significant variation of temperature and pH during the degradation of PFOA by FAC/PMS or NAC/PMS. To this end, DFT calculations were used to verify the proposed assumption and provided useful insights into the adsorption effect, which was also a rate-limiting step during the degradation process of PFOA. The FAC and NAC can concentrate the PFOA in soil which proves helpful for the proceeding catalytic oxidation. Therefore, thermally-activated PMS coupled with FAC/NAC can be a promising decomposition technique with significant potential for the in-situ remediation of PFOA-contaminated sites.

Acknowledgements

This research was supported by National Key Research and Development Program of China (No. 2019YFC1803701), National Natural Science Foundation of China (No. 51708223) and we acknowledge the Chinese Scholarship Council of PR China for providing financial support for Guanhong Liu to stay at the ENSCR.

References

- [1] Giesy, J.P., Kannan, K., 2001. Global distribution of perfluorooctane sulfonate in wildlife. *Environ. Sci. Technol.* 35, 1339-1342.
- [2] Kannan, K., Corsolini, S., Falandysz, J., Fillmann, G., Kumar, K.S., Loganathan, B.G., Mohd, M.A., Olivero, J., Wouwe, N.V., Yang, J.H., 2004. Perfluorooctanesulfonate and related fluorochemicals in human blood from several countries. *Environ. Sci. Technol.* 38, 4489-4495.
- [3] Jensen, A.A., Leffers, H., 2008. Emerging endocrine disruptors: perfluoroalkylated substances. *Int. J. Androl.* 31, 161-169.
- [4] Qu, Y., Zhang, C.J., Li, F., Chen, J., Zhou, Q., 2010. Photo-reductive defluorination of

perfluorooctanoic acid in water. *Water. Res.* 44, 2939-2947.

[5] Kennedy, G.L., Butenhoff, J.L., Olsen, G.W., O'Connor, J.C., Seacat, A.M., Perkins, R.G., Biegel, L.B., Murphy, S.R., Farrar, D.G., 2004. The toxicology of perfluorooctanoate. *Crit. Rev. Toxicol.* 34, 351-384.

[6] Lyu, Y., Brusseau, M.L., Chen, W., Yan, N., Fu, X.R., Lin, X.Y., 2018. Adsorption of PFOA at the air-water interface during transport in unsaturated porous media. *Environ. Sci. Technol.* 52, 7745-7753.

[7] Murakami, M., Kurdoda, K., Sato, N., Fukushi, T., Takizawa, S., Takada, H., 2009. Groundwater pollution by perfluorinated surfactants in Tokyo. *Environ. Sci. Technol.* 43, 3480-3486.

[8] Sorengård, M., Niarchos, G., Jensen, P.E., Ahrens, L., 2019. Electrolytic per- and polyfluoroalkyl substances (PFASs) removal mechanism for contaminated soil. *Chemosphere* 232, 224-231.

[9] Sinclair, E., Kannan, K., 2006. Mass loading and fate of perfluoroalkyl surfactants in wastewater treatment plants. *Environ. Sci. Technol.* 40, 1408-1414.

[10] Ahrens, L., Taniyasu, S., Yeung, L.W., Yamashita, N., Lam, P.K., Ebinghaus, R., 2010. Distribution of polyfluoroalkyl compounds in water, suspended particulate matter and sediment from Tokyo Bay, Japan. *Chemosphere* 79, 266-272.

[11] Yan, H., Zhang, C.J., Zhou, Q., Chen, L., Meng, X.Z., Short-and long-chain perfluorinated acids in sewage sludge from Shanghai, China. *Chemosphere* 88(2012)1300-1305.

[12] Gan, C.D., Gan, Z.W., Cui, S.F., Fan, R.J., Fu, Y.Z., Peng, M.Y., Yang, J.Y., Agricultural activities impact on soil and sediment fluorine and perfluorinated compounds in an endemic fluorosis area, *Sci. Total Environ.* 771 (2021) 144809-144816.

[13] He, Y., Zeng, F.F., Lian, Z.H., Xu, J.M., Brookes, P.C., 2015. Natural soil mineral nanoparticles are novel sorbents for pentachlorophenol and phenanthrene removal. *Environ. Pollut.* 205, 43-51.

[14] Liu, G.H., Stewart B.A., Yuan K., Ling S.Y., Zhang, M., Wang, G.J., Lin, K.F., 2021. Comprehensive adsorption behavior and mechanism of PFOA and PFCs in various subsurface systems in China. *Sci. Total Environ.* 794, 148463-148473.

[15] Yang, L., He, L.Y., Xue, J.M., Ma, Y.F., Xie, Z.Y., Wu, L., Huang, M., Zhang, Z.L., 2021. Persulfate-based degradation of perfluorooctanoic acid (PFOA) and perfluorooctane sulfonate (PFOS) in aqueous solution: review on influences, mechanisms and prospective. *J. Hazard. Mater.* 393, 122405-122415.

- [16] Turner, B.D., Sloan, S.W., Currell, G.R., 2019. Novel remediation of per- and polyfluoroalkyl substances (PFASs) from contaminated groundwater using cannabis sativa L. (hemp) protein powder. *Chemosphere* 229, 22-31.
- [17] Liu, J.Q., Xiang, W.R., Li, C.G., Hoomissen, D.G.V., Qi, Y.M., Wu, N.N., Al-Basher, G., Qu, R.J., Wang, Z.Y., 2021. Kinetics and mechanism analysis for the photodegradation of PFOA on different solid particles. *Chem. Eng. J.* 383, 123115-123121.
- [18] Sammut, G., Sinagra, E., Sapiano, M., Helmus, R., Voogt, P.D., 2019. Perfluoroalkyl substances in the Maltese environment - (II) sediments, soils and groundwater. *Sci. Total Environ.* 682, 180-189.
- [19] Turner, L.P., Kueper, B.H., Jaansalu, K.M., Patch, D.J., Battye, N., El-Sharnouby, O., Mumford, K.G., Weber, K.P., 2021. Mechanochemical remediation of perfluorooctanesulfonic acid (PFOS) and perfluorooctanoic acid (PFOA) amended sand and aqueous film-forming foam (AFFF) impacted soil by planetary ball milling, *Sci. Total Environ.* 765, 1-10.
- [20] Sørmo, E., Silvani, L., Bjerkli, N., Hageman, N., Zimmerman, A. R., Hale, S. E., Hansen, C. B., Hartnik, T., Cornelissen, G. 2020. Stabilization of PFAS-contaminated soil with activated biochar. *Sci. Total Environ.* 144034-144044.
- [21] Du, Z., Deng, S., Bei, Y., Huang, Q., Wang, B., Huang, J., Yu, G., 2014. Adsorption behavior and mechanism of perfluorinated compounds on various adsorbents-a review. *J. Hazard. Mater.* 274, 443-454.
- [22] Peng, Y.P., Chen, H.L., Huang, C.P., 2017. The synergistic effect of photoelectrochemical (PEC) reactions exemplified by concurrent perfluorooctanoic acid (PFOA) degradation and hydrogen generation over carbon and nitrogen co-doped TiO₂ nanotube arrays (CN-TNTAs) photoelectrode. *Appl. Catal. B-Environ.* 209, 437-446.
- [23] Liu, Y.M., Chen, S., Quan, X., Yu, H.T., Zhao, H.M., Zhang, Y.B., 2015. Efficient mineralization of perfluorooctanoate by electro-Fenton with H₂O₂ electro-generated on hierarchically porous carbon. *Environ. Sci. Technol.* 49, 13528-13533.
- [24] Devi, P., Das, U., Dalai, A.K., 2016. In-situ chemical oxidation: principle and applications of peroxide and persulfate treatments in wastewater systems. *Sci. Total Environ.* 571, 643-657.
- [25] Khalil, L.B., Girgis, B.S., Tawfik, T.A., 2001. Decomposition of H₂O₂ on activated carbon obtained from olive stones. *J. Appl. Chem. Biotechnol.* 76, 1132-1140.

- [26] Yun, E.T., Moon, G.H., Lee, H.S., Jeon, T., Lee, C.H., Choi, W., Lee, J., 2018. Oxidation of organic pollutants by peroxymonosulfate activated with low temperature-modified nanodiamonds: understanding the reaction kinetics and mechanism. *Appl. Catal. B-Environ.* 237, 432-441.
- [18] Wang, J.L., Wang, S.Z., 2018. Activation of persulfate (PS) and peroxymonosulfate (PMS) and application for the degradation of emerging contaminants. *Chem. Eng. J.* 334, 1502-1517.
- [27] Liu, J.Q., Qu, R.J., Wang, Z.Y., Mendoza-Sanchez, I., Sharma, V.K., 2017. Thermal-and photo-induced degradation of perfluorinated carboxylic acids: kinetics and mechanism. *Water. Res.* 126, 12-18.
- [28] Chen, M.J., Lo, S.L., Lee, Y.C., Huang, C.C., 2015. Photocatalytic decomposition of perfluorooctanoic acid by transition-metal modified titanium dioxide. *J. Hazard. Mater.* 288, 168-175.
- [29] Da Silva-Rackov, C.K.O., Lawal, W.A., Nfodzo, P.A., Vianna, M.M.G.R., Do Nascimento, C.A.O., Choi, H., 2016. Degradation of PFOA by hydrogen peroxide and persulfate activated by ironmodified diatomite. *Appl. Catal. B-Environ.* 192, 253-259.
- [30] Qian, Y.J., Guo, X., Zhang, Y.L., Peng, Y., Sun, P.Z., Huang, C.H., Niu, J.F., Zhou, X.F., Crittenden, J.C., 2016. Perfluorooctanoic acid degradation using UV/persulfate process: modeling of the degradation and chlorate formation. *Environ. Sci. Technol.* 50, 772-781.
- [31] Tsitonaki, A., Petri, B., Crimi, M., Mosbaek, H., Siegrist, R.L., Bjerg, P.L., 2010. In situ chemical oxidation of contaminated soil and groundwater using PS: a review, *Crit. Rev. Environ. Sci. Technol.* 40, 55-91.
- [32] Peter, L.O., DeSutter, T.M., Casey, F.X.M., Khan, E., Wick, A.F., 2018. Thermal remediation alters soil properties - a review. *J. Environ. Manage.* 206, 826-835.
- [33] Antoniou, M.G., Cruz, A.A.D.L., Dionysiou, D.D., 2010. Degradation of microcystin-LR using sulfate radicals generated through photolysis, thermolysis and e-transfer mechanisms. *Appl. Catal. B-Environ.* 96, 290-298.
- [34] Wang, L., Peng, L., Xie, L., Deng, P., Deng, D., 2017. Compatibility of surfactants and thermally activated prsulfate for enhanced subsurface remediation. *Environ. Sci. Technol.* 51, 7055-7064.
- [35] Liu, G.H., Li, C., Stewart, B.A., Liu, L., Zhang, M., Yang, M., Lin, K.F., 2020b. Enhanced thermal activation of peroxymonosulfate by activated carbon for efficient removal of perfluorooctanoic acid. *Chem.*

Eng. J. 399, 125722-125731.

[36] Peng, H.J., Zhang, W., Liu, L., Lin, K. F., 2017. Degradation performance and mechanism of decabromodiphenyl ether (BDE209) by ferrous-activated persulfate in spiked soil. Chem. Eng. J. 307, 750-755.

[37] Chen, S., Jiao, X.C., Gai, N., Li, X.J., Wang, X.C., Lu, G.H., Piao, H.T., Rao, Z., Yang, Y.L., 2016. Perfluorinated compounds in soil, surface water, and groundwater from rural areas in eastern China. Environ. Pollut. 211, 124-131.

[38] Liu, G.H., Feng, M.Y., Tayyab, M., Gong, J.Q., Zhang, M., Yang, M.Y., Lin K.F., 2021. Direct and efficient reduction of perfluorooctanoic acid using bimetallic catalyst supported on carbon. J. Hazard. Mater. 412, 125224-125233.

[39] Köster, D., Jochmann, M.A., Lutze, H.V., Schmidt, T.C., 2019. Monitoring of the total carbon and nitrogen balance during the mineralization of nitrogen containing compounds by heat activated persulfate. Chem. Eng. J. 367, 160-168.

[40] Delley, B. 2000. From molecules to solids with the DMol3 approach. J. Chem. Phys. 113 (18), 7756-7764.

[41] Hammer, B., Hansen, L.B., Nørskov, J.K. 1999. Improved adsorption energetics within density-functional theory using revised Perdew-Burke-Ernzerhof functionals. Phys. Rev. B 59 (11), 7413-7421.

[42] Methfessel, M., Paxton, A.T. 1989. High-precision sampling for Brillouin-zone integration in metals. Phys. Rev. B 40 (6), 3616-3621.

[43] Chadi, D.J. 1977. Special points for Brillouin-zone integrations. Phys. Rev. B 16 (4), 1746-1747.

[44] Forouzes, M., Ebadi, A., Aghaeinejad-Meybodi, A., Khoshbouy, R., 2019. Transformation of persulfate to free sulfate radical over granular activated carbon: effect of acidic oxygen functional groups. Chem. Eng. J. 374, 965-974.

[45] H. Hori, Y. Nagaoka, M. Murayama, S. Kutsuna, Efficient decomposition of perfluorocarboxylic acids and alternative fluorochemical surfactants in hot water, Environ. Sci. Technol. 42 (2008) 7438-7443.

[46] Qi, Y.M., Qu, R.J., Liu, J.Q., Chen, J., Al-Basher, G., Alsultan, N., Wang, Z.Y., Huo, Z.L., 2019. Oxidation of flumequine in aqueous solution by UV-activated peroxymonosulfate: Kinetics, water matrix

effects, degradation products and reaction pathways, *Chemosphere* 237, 124484-124493.

[47] Wang, J., Duan, X.G., Gao, J., Shen, Y., Fen, X.H., Yu, Z.J., Tan X.Y., Liu, S.M., Wang, S.B., 2020. Roles of structure defect, oxygen groups and heteroatom doping on carbon in nonradical oxidation of water contaminants, *Water Res.* 185, 116244-116254.

[48] Song, W., Li, J., Fu, C.X., Wang, Z.Y., Zhang, X.L., Yan, J.X., Hogland, W., Gao, L. 2019. Kinetics and pathway of atrazine degradation by a novel method: Persulfate coupled with dithionite. *Chem. Eng. J.* 373, 803-813.

[49] Li, H.C., Qian, J.S., Pan, B.C., 2021. N-coordinated Co containing porous carbon as catalyst with improved dispersity and stability to activate peroxydisulfate for degradation of organic pollutants. *Chem. Eng. J.* 403, 126395-126403.

[50] Duan, P.J., Liu, X.N., Liu, B.H., Akra, M., Li, Y.W., Pan, J.W., Yue, Q.Y., Gao, B.Y., Xu, X., 2021. Effect of phosphate on peroxydisulfate activation: Accelerating generation of sulfate radical and underlying mechanism. *Appl. Catal. B-Environ.* 298, 120532-120541.

[51] Jiang, W.C., Tang, P., Lu, S.G., Xue, Y.F., Zhang, X., Qiu, Z.F., Sui, Q., 2018. Comparative studies of H₂O₂/Fe(II)/formic acid, sodium percarbonate/Fe(II)/formic acid and calcium peroxide/Fe(II)/formic acid processes for degradation performance of carbon tetrachloride. *Chem. Eng. J.* 344, 453-461.

[52] Neta, P., Huie, R.E., Ross, A.B., 1988. Rate constants for reactions of inorganic radicals in aqueous solution. *J. Phys. Chem. Ref. Data.* 17, 1027-1284.

[53] Wang, N., Lv, H.Q., Zhou, Y.Q., Zhu, L.H., Hu, Y., Majima, T., Tang, H.Q., 2019. Complete defluorination and mineralization of perfluorooctanoic acid by a mechanochemical method using alumina and persulfate. *Environ. Sci. Technol.* 53, 8302-8313.

[54] Yuan, C., Huang, Y., Cannon, F.S., Geng, C., Liang, Z., Zhao, Z., 2020. Removing PFOA and nitrate by quaternary ammonium compounds modified carbon and its mechanisms analysis: Effect of base, acid or oxidant pretreatment, *Chemosphere.* 242, 125233-155243.

[55] Zhang, Y., Moores, A., Liu, J., Ghoshal, S., 2019. New Insights into the Degradation Mechanism of Perfluorooctanoic Acid by Persulfate from Density Functional Theory and Experimental Data, *Environ. Sci. Technol.* 53, 8672-8681.

Figure Captions

Fig. 1. PFOA degradation performance in the presence of FAC/PMS or NAC/PMS in thermal activated oxidation process in soils, where temperature ranges from 25 - 80 °C. ($[PFOA]_0 = 1.0$ mg/kg, $[PMS] = 5.0$ mM, $[FAC] = [NAC] = 4.0$ g/L).

Fig. 2. (a) The influence of PMS dosage on the PFOA removal in soil at 60 °C ($[PFOA]_0 = 0.7$ mg/kg, soil: PMS solution = 1.0 g/1 mL, 5 h). Effects of FAC (b) and NAC (c) on the PFOA removal in soil, where the soil is nature dried soil and soil-600 represents the soil without organic carbon after 600 °C burning. (The light blue lines represent the removal rate of PFOA in aqueous) (Reaction of b and c: $[PFOA]_0 = 0.8$ mg/kg, soil: solution containing various amount of AC = 1.0 g/1 mL, 5 h, 60 °C). (d) The PFOA removal in the presence of FAC or NAC alone in soils as the function of time ($[PFOA]_0 = 0.7$ mg/kg, AC = 8 g/L, 60 °C).

Fig. 3. (a) The relationship between PFOA removal efficiency and the same chemical agent dissolved in different solution volumes. ($[PFOA]_0 = 0.7$ mg/kg, soil = 1.0 g, AC = 8 g/L, 60 °C). (b) The degradation of PFOA in soils by using FAC/PMS or NAC/PMS as the function of time ($[PFOA]_0 = 0.5$ mg/kg, PMS = 15 mM, AC = 8 g/L, the ratio of soil and solution = 1.0 g/ 1 mL, 60 °C).

Fig. 4. PFOA degradation over a pH range of 3.0 - 9.0 in the presence of FAC/PMS or NAC/PMS in soil. ($[PFOA]_0 = 1.0$ mg/kg, PMS = 15 mM, AC = 8 g/L, the ratio of soil and solution = 1.0 g/ 1 mL, 60 °C)

Fig. 5. Effects of coexisting ions and organic matter on PFOA degradation efficiency of FAC/PMS (a) and NAC/PMS (b) in soil. ($[PFOA]_0 = 1.0$ mg/kg, PMS = 15 mM, AC = 8 g/L, the ratio of soil and solution = 1.0 g/ 1 mL, 60 °C, reaction time: 6 h)

Fig. 6. (a) F^- as a function of time and (b) Mass balance of F^- during catalytic-oxidation degradation of PFOA at 60 °C. (a and b: $[PFOA]_0 = 1.0$ mg/kg and the pH was not buffered. The columns from left to right are FAC/PMS and NAC/PMS in soil, and FAC/PMS and NAC/PMS in soil-600 in 1 h and 12 h. The grey, orange and cyan sections respectively represent undegraded PFOA, remained short-chain PFOA and produced F ions.)

Fig. 7. FTIR spectra of primary FAC, soil and the mixture of NS/FAC after reaction.

Fig. 8. Solid phase molecule configurations of a) FAC, b) NAC and c) SiO_2 bonded with PFOA. (The red, white, grey, blue, cyan, and yellow spheres indicate O, H, C, N, F and Si atom, respectively.)

Supplement

Table. S1 Matrix spike recovery percentage of target PFCAs in soil.

Table S1. Detailed information of the detected short-chained PFCAs compound.

Table S3. The effect of temperature on moisture content in soil.

Table. S4 Textural properties of FAC and NAC.

Fig.S1. PFOA degradation performance in the presence of PMS alone in thermal activated oxidation process in aqueous, where temperature ranges from 60 - 100 °C. ($[PFOA]_0 = 1.0 \text{ mg/L}$, $[PMS] = 5.0 \text{ mM}$, $[FAC] = [NAC] = 4.0 \text{ g/L}$).

Fig.S2. (a) Effect of radical scavenger (methanol) on PFOA degradation in soil. (b) EPR spectra of sulfate radicals and hydroxyl radicals in different scenarios. ($[PFOA]_0 = 1.0 \text{ mg/kg}$, $PMS = 15 \text{ mM}$, $FAC/NAC = 8 \text{ mg/L}$, $V_{PFOA}/V_{MeOH} = 1:1$, $T = 60 \text{ }^\circ\text{C}$.)

Fig. S3 HPLC-MS/MS identified intermediates products of PFOA yielded after thermal activated AC/PMS.

Fig. S4 The XRD pattern of the SiO_2 in soil.

Fig. 1.

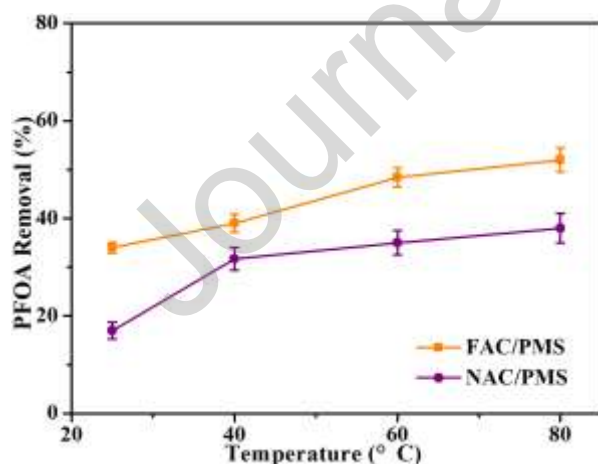


Fig.1. PFOA degradation performance in the presence of FAC/PMS or NAC/PMS in thermal activated oxidation process in soils, where temperature ranges from 25 - 80 °C. ($[PFOA]_0 = 1.0 \text{ mg/kg}$, $[PMS] = 5.0 \text{ mM}$, $[FAC] = [NAC] = 4.0 \text{ g/L}$).

Fig. 2.

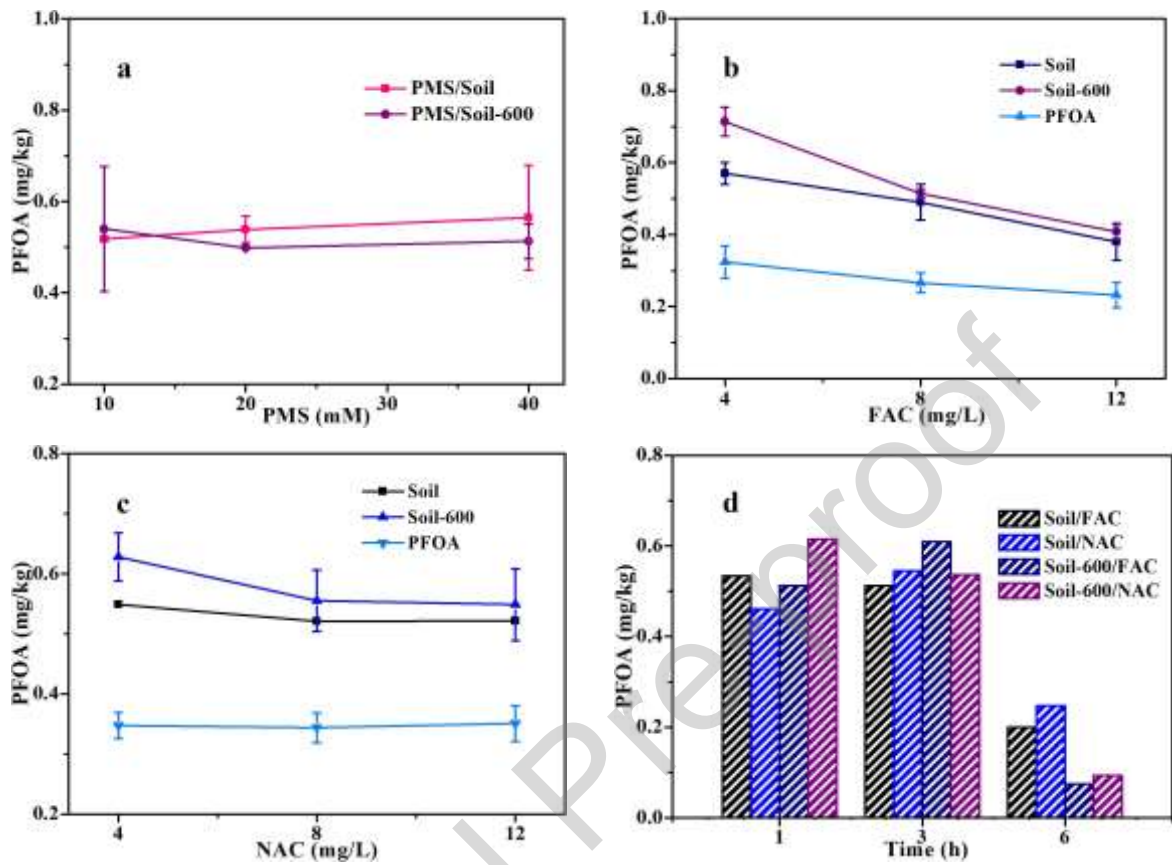


Fig. 2. (a) The influence of PMS dosage on the PFOA removal in soil at 60 °C ($[PFOA]_0 = 0.7$ mg/kg, soil: PMS solution = 1.0 g/1 mL, 5 h). Effects of FAC (b) and NAC (c) on the PFOA removal in soil, where the soil is nature dried soil and soil-600 represents the soil without organic carbon after 600 °C burning. (The light blue lines represent the removal rate of PFOA in aqueous) (Reaction of b and c: $[PFOA]_0 = 0.8$ mg/kg, soil: solution containing various amount of AC = 1.0 g/1 mL, 5 h, 60 °C). (d) The PFOA removal in the presence of FAC or NAC alone in soils as the function of time ($[PFOA]_0 = 0.7$ mg/kg, AC = 8 g/L, 60 °C)

Fig. 3.

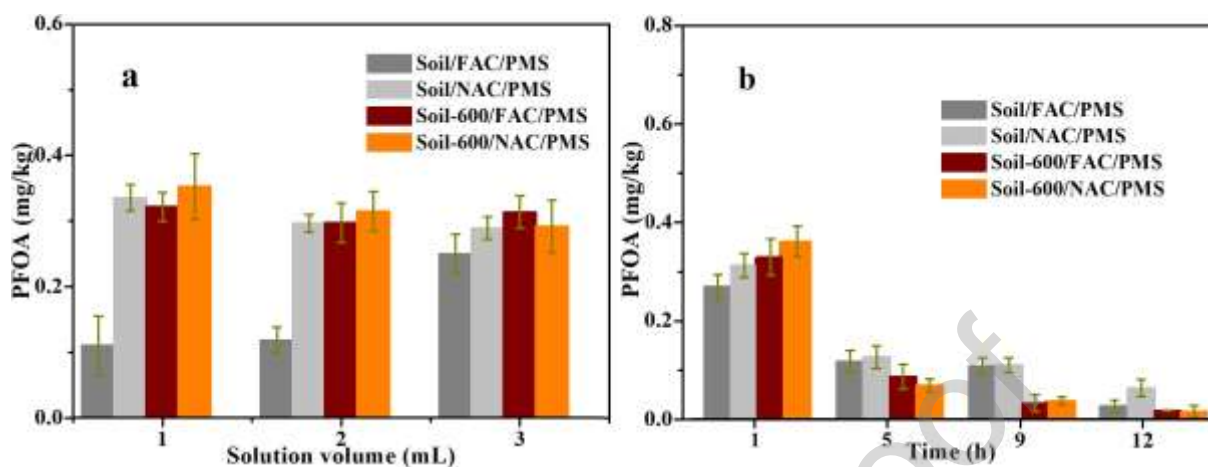


Fig. 3. (a) The relationship between PFOA removal efficiency and the same chemical agent dissolved in different solution volumes. ($[PFOA]_0 = 0.7$ mg/kg, soil = 1.0 g, AC = 8 g/L, 60 °C). (b) The degradation of PFOA in soils by using FAC/PMS or NAC/PMS as the function of time ($[PFOA]_0 = 0.5$ mg/kg, PMS = 15 mM, AC = 8 g/L, the ratio of soil and solution = 1.0 g/ 1 mL, 60 °C).

Fig. 4.

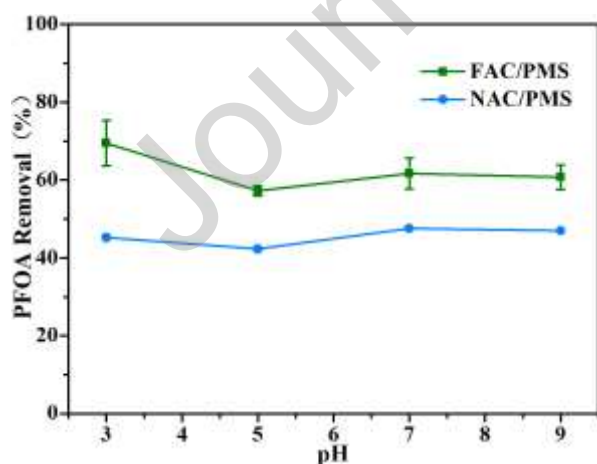


Fig. 4. PFOA degradation over a pH range of 3.0-9.0 in the presence of FAC/PMS or NAC/PMS in soil. ($[PFOA]_0 = 1.0$ mg/kg, PMS = 15 mM, AC = 8 g/L, the ratio of soil and solution = 1.0 g/ 1 mL, 60 °C)

Fig. 5.

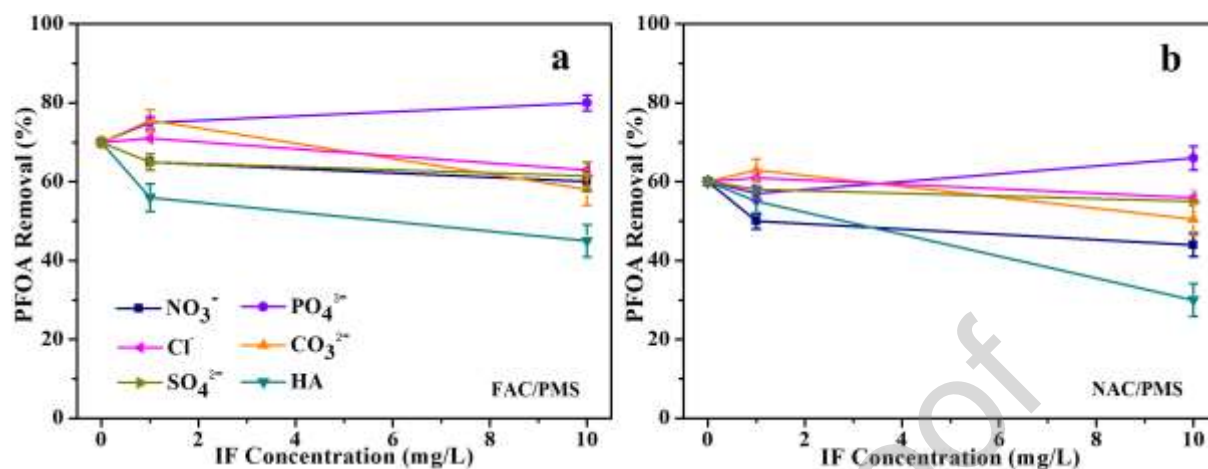


Fig. 5. Effects of coexisting ions and organic matter on PFOA degradation efficiency of FAC/PMS (a) and NAC/PMS (b) in soil. ($[PFOA]_0 = 1.0$ mg/kg, PMS = 15 mM, AC = 8 g/L, the ratio of soil and solution = 1.0 g/ 1 mL, 60 °C, reaction time: 6 h)

Fig. 6.

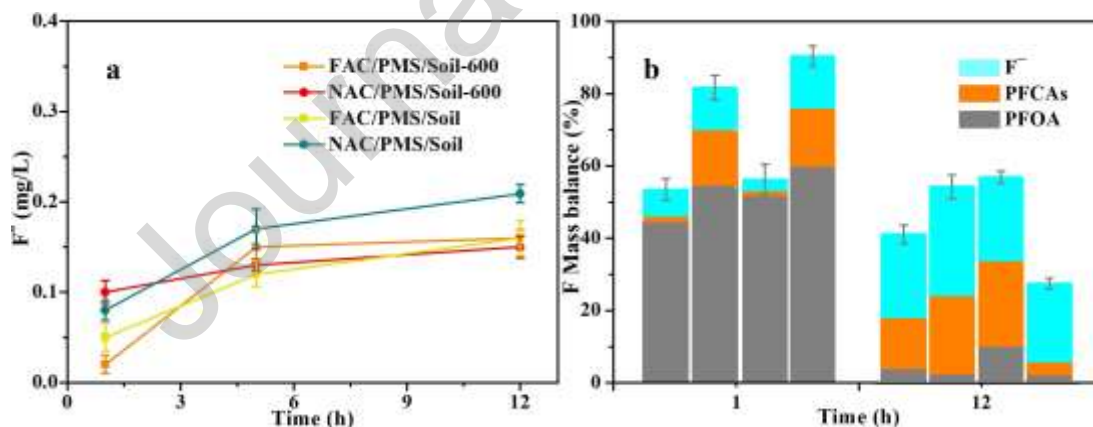


Fig. 6. (a) F^- as a function of time and (b) Mass balance of F^- during catalytic-oxidation degradation of PFOA at 60 °C. (a and b: $[PFOA]_0 = 1.0$ mg/kg and the pH was not buffered. The columns from left to right are FAC/PMS and NAC/PMS in soil, and FAC/PMS and NAC/PMS in soil-600 in 1 h and 12 h. The grey, orange and cyan sections respectively represent undegraded PFOA, remained short-chain PFOA and produced F^- ions.)

Fig. 7.

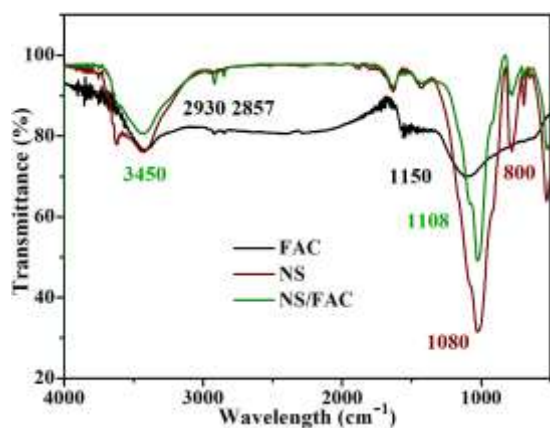


Fig. 7. FTIR spectra of primary FAC, soil and the mixture of NS/FAC after reaction.

Fig. 8.

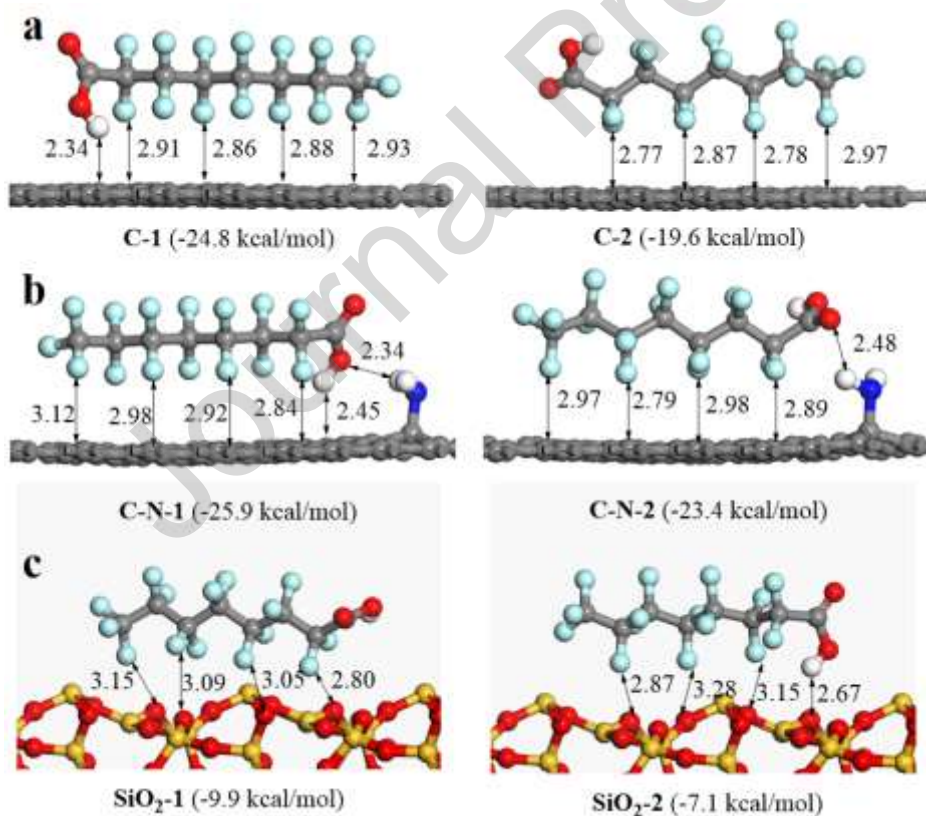
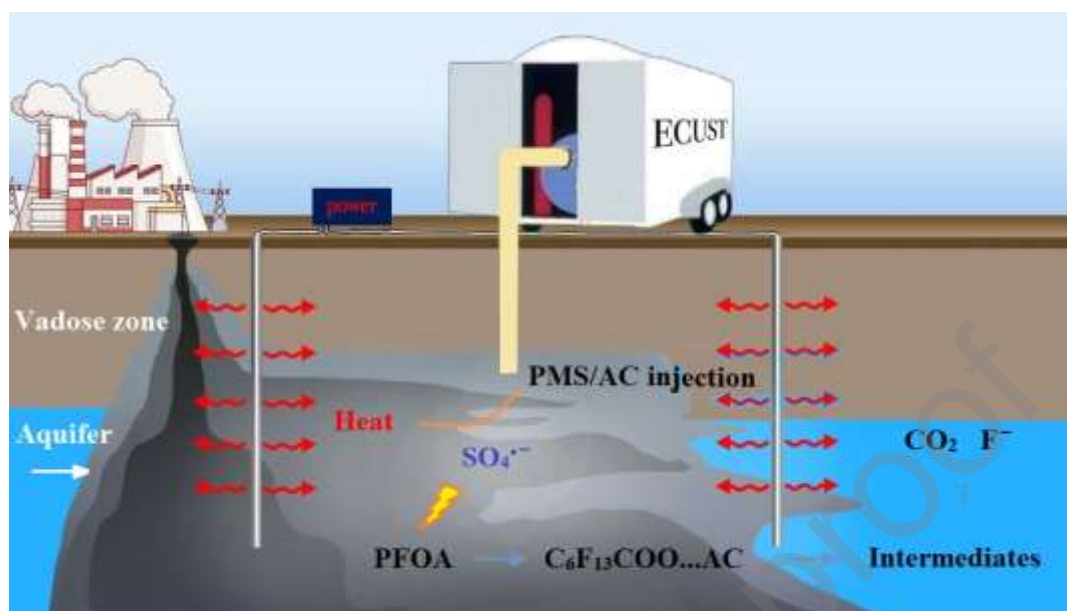


Fig. 8. Solid phase molecule configurations of a) FAC, b) NAC and c) SiO_2 bonded with PFOA. (The red, white, grey, blue, cyan, and yellow spheres indicate O, H, C, N, F and Si atom, respectively.)

Graphical abstract



CRediT authorship contribution statement

Guanhong Liu: Conceptualization; Experiment; Data curation; Formal analysis; Draft writing

Jiahao Qian: Experiment; Data curation; Formal analysis

Zhang Yu: Experiment; Calculation

Kuangfei Lin: Conceptualization; Funding acquisition; Supervision

Fuwen Liu: Validation; Funding acquisition

Declaration of interests

The authors declare that they have no known competing financial interests or personal relationships that could have appeared to influence the work reported in this paper.

The authors declare the following financial interests/personal relationships which may be considered as potential competing interests:

Highlights

- Thermal assisted heterogeneous activation of PMS by AC was applied in PFOA contaminated soil remediation.
- Soil structure has buffering properties against external factors which in turn reduces removal efficiency.
- PFOA contaminated soil with lower OC consumes less adsorbent and oxidant during the remediation.
- DFT calculations revealed that adsorption strength of AC on PFOA was 3.5 times higher than soil's.